# Fabrication and Characterization of Fe-Pd Ferromagnetic Shape-Memory Thin Films

Yuki Sugimura, Tzahi Cohen-Karni, Patrick McCluskey and Joost Vlassak
Division of Engineering and Applied Sciences, Harvard University,
Cambridge, MA 02138, U.S.A.

## ABSTRACT

Fe-Pd thin films with approximately 30 at.% Pd have been produced by magnetron sputtering. Various heat treatment conditions were studied in order to obtain the face-centered tetragonal (fct) martensitic phase at room temperature. X-ray diffractometry was used to identify the various phases present at room temperature and the substrate curvature technique was employed to measure film stress as a function of temperature. The shape memory effect was demonstrated in samples containing the fct martensite phase at room temperature.

## INTRODUCTION

Ferromagnetic shape memory materials have received attention recently because large strains can be achieved by the application of an external magnetic field. The mechanism by which strain is obtained in the magnetic shape memory effect (MSME) differs from that in magnetostriction. In magnetostriction strain is induced upon rotation of magnetic moment in each magnetic domain. On the other hand, the magnetic shape memory effect is achieved by conversion of martensite variants through twin boundary motion so that the new crystal orientation allows the magnetic moment to be better aligned with the external magnetic field. MSME has already been demonstrated in the Ni-Mn-Ga systems [1-4], ordered $Fe_3Pt$ [4,5], and disordered Fe-Pd alloys [4,6-10] in bulk form. However, only a limited amount of research has been conducted on Fe-Pd thin films [11-14].

In bulk $Fe_{x-1}Pd_x$ alloys the transformation from the parent face-centered cubic (fcc) phase to the face-centered tetragonal (fct) martensite phase occurs at x ~0.3. The martensite start temperature, $M_s$, is typically below room temperature and decreases rapidly with increasing Pd content [7]. Inoue et al. [13,14], however, have shown that the $M_s$ of Fe-Pd alloys increases to above room temperature in thin film form, and that fct martensite can be obtained at room temperature at x ~0.28.

In this study Fe-Pd thin films with a variation in Pd content are obtained by magnetron sputtering. The effect of post-deposition heat treatment on the crystal structure is investigated using x-ray diffraction. The shape memory effect is demonstrated in films with fct martensite by using the substrate curvature method during thermal cycles.

## EXPERIMENTAL DETAILS

Fe-Pd thin films were deposited by magnetron sputtering in a high vacuum chamber equipped with multiple confocal guns (ATC 1800, AJA International). The sputtering configuration is schematically shown in Figure 1. Previous studies by other researchers on Fe-Pd

thin films sputtered from Fe-30 at.% Pd alloy targets consistently showed a deficiency in the Pd content of the sputtered film [11-13]. Therefore, elemental Fe and elemental Pd targets were selected in order to avoid this problem. The use of elemental targets also provides a simple way of producing films with various compositions. All the films were deposited on either 150 nm-thick thermally grown oxide (TGO) on 500 μm-thick (100) Si or 200 nm-thick $SiN_x$ on 200 μm-thick (100) Si wafers. The base chamber pressure was typically below 1.7 x $10^{-7}$ Torr, and the Ar working gas pressure was 5 mTorr. The substrate was rotated at a speed of 17 revolutions per minute to maximize thickness and compositional uniformity. The gun tilt angle $\phi$ was fixed at $21^{o}$ and the working distance, WD, was maintained at approximately 100 mm for all the deposition runs. The power applied to the Fe target and the Pd target was varied between 200-320 W and 30-54 W, respectively. Film thickness and composition were analyzed with Rutherford Backscattering Spectrometry (RBS), using a 1.7 MV General Ionex Tandetron Accelerator equipped with both a gas and a heavy ion source.

Sputtered films in the as-deposited condition often consist of very fine grains and require post deposition heat treatment. All the heat treatments were conducted at $900^{o}$C while other heat treatment parameters such as time, ambient and the cooling method were varied in order to obtain the metastable fct martensite at room temperature. The crystal structure of the film was analyzed by x-ray diffraction (XRD) using a Philips PW1010 diffractometer (Cu $K_{\alpha}$ radiation). The film surface morphology was observed using a LEO 982 scanning electron microscope (SEM). Heat-treated films were ferromagnetic as demonstrated by their interaction with a permanent magnet.

The shape memory effect was investigated by measuring the development of film stress as a function of temperature. Substrate curvature method was used to monitor the changes in sample curvature under thermal cycling between 15-$200^{o}$C. The Stoney Formula was used to convert curvature into film stress.

## RESULTS AND DISCUSSION

Figure 2 shows the variation in Pd content in the as-deposited film as a function of power

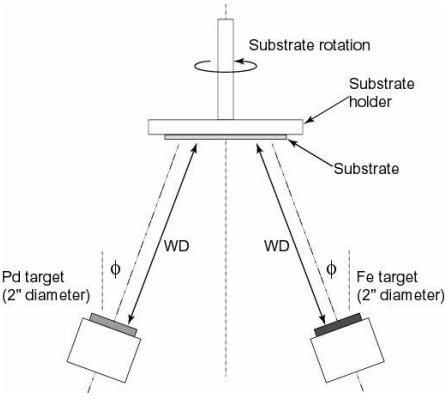


**Figure 1.** Schematic of sputtering from multiple confocal guns using elemental Fe and Pd targets.

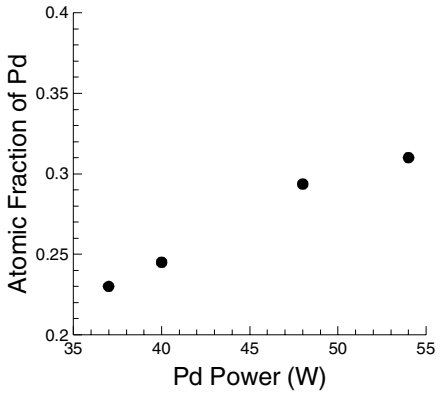


**Figure 2.** Variation of Pd content in the as-deposited film as a function of power applied to Pd target. The power applied to Fe target is fixed at 320 W.

applied to the Pd target while the power on the Fe target was fixed at 320 W. There is a linear increase in Pd content as the power is raised. The desired Pd atomic fraction of ~0.28 is achieved at 48 W Pd. The thickness of the film varied between 300 nm (deposition time, *t*, of 20 minutes) and 1,100 nm (*t* = 60 minutes). Film thickness uniformity was typically ~2.5% and compositional variation was typically less than 0.5 at.% over 100 mm. SEM and XRD revealed that the as-deposited films typically consist of nanocrystalline grains in the body-centered cubic (bcc) structure.

Figure 3 shows the effect of various heat treatment conditions on the room temperature phases in Fe-28.3 at.% Pd film. The heat treatments were performed in a vacuum furnace with a base pressure of less than 5 x $10^{-6}$ Torr. Significant levels of oxidation are observed in the sample heat treated in vacuum for 65 minutes and quenched in ice water. Sample oxidation may have occurred due to residual oxygen in the furnace. However, oxidation may also have occurred when the sample was taken out of the furnace for quenching in ice water. Oxidation is suppressed when the specimens were heated in flowing, oxygen-gettered Ar and then rapidly cooled in flowing Ar. Iron oxide peaks are noticeably absent and distinct (111) fcc and (220) fcc peaks can be seen. When the sample is heat treated for 60 minutes in flowing Ar, there is a sharp (200) fcc peak. When the heat treatment time is reduced to 15 minutes there is a broadening of the (200) peak at 2θ ~49°. This peak broadening is an indication that the fcc austenite has started to transform into the fct martensite. Therefore, a short heat treatment time in flowing oxygen-gettered Ar followed by rapid cooling in flowing Ar seems to produce the desired crystal structure. This method minimizes oxidation of the film as well as the compositional changes that may result from any reaction products that can form at the film-substrate interface at high temperatures and long annealing times. Furthermore, an annealing time of 15 minutes seems to be sufficient to convert the bcc structure of the as-deposited films to the fcc structure during annealing. Therefore, heat treatments of all subsequent samples were conducted in flowing oxygen-gettered Ar for 15 minutes at 900°C then rapidly cooled in flowing Ar.

Figure 4 shows the different crystal structures obtained as the Pd content is varied from 26.52% to 30%. All the samples were heat treated at 900°C for 15 minutes in flowing, oxygen-

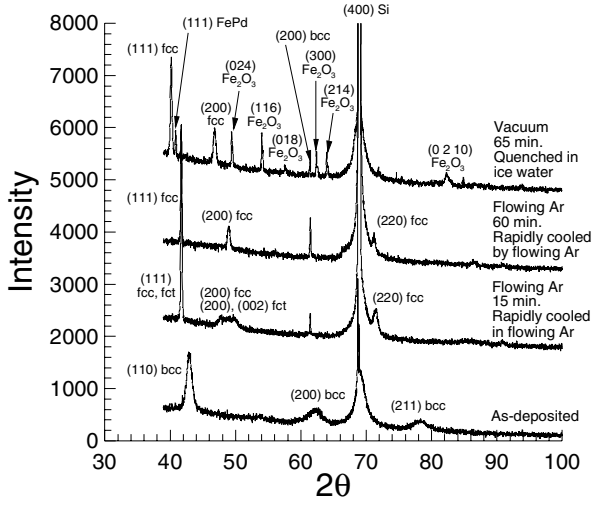


**Figure 3.** Effect of heat treatment at 900°C on crystal structure (28.3 at.% Pd). Film thickness is 588 nm

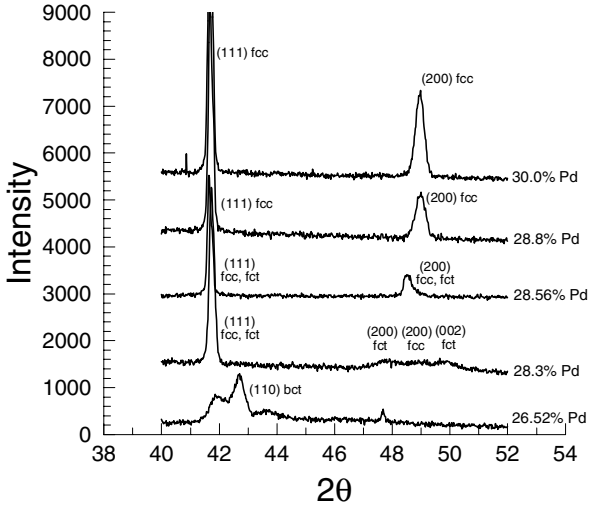


**Figure 4.** Room temperature phases as a function of Pd content.

getterd Ar followed by rapid cooling by flowing Ar. When the Pd content is high the film consists of the fcc parent phase only. As the Pd content is decreased the fcc parent phase begins to transform to the fct martensite as indicated by a shift and broadening of the (200) peak. At the lowest Pd level the crystal structure further breaks down into the body centered tetragonal (bct) structure shown by the splitting of the (111)fcc peak into the (110)/(101) bct peaks.

Figure 5 shows an SEM micrograph of the surface of a heat treated sample (film thickness = 580 nm) containing 28.8 at.% Pd. The grain size is on the order of 1 to 2 μm, which is significantly larger than the grain size expected for a thin film whose thickness is 580 nm. There is a distinct formation of steps or ledges on the film surface. A similar surface morphology is observed by Inoue et al. [14] in heat treated films containing fct martensite with a grain size of 2 to 4 μm.

Changes in film stress as a function of temperature for Fe-Pd films containing the fct martensite are shown in Figures 6 and 7. In the sample with a higher Pd content (Figure 6) there is a linear increase in film stress as the temperature is raised. At about 65$^{o}$C the slope of the curve changes and the film stress continues to increase linearly. Upon cooling the stress decreases, following the heating curve in the reverse direction. At about 45$^{o}$C the slope begins to change, and at about 30$^{o}$C the stress drops off rapidly with decreasing temperature. Although not shown in the figure, it is presumed that the film stress continues to decrease with decreasing temperature until transformation from the fcc phase to the fct martensite is complete. Figure 7 shows the variation of film stress under thermal cycling in an Fe-Pd film containing a slightly lower Pd content. In general, the transformation temperature has increased compared to the sample with a higher Pd content. Upon heating transformation from fct to fcc begins and is completed at approximately 80$^{o}$C. Upon cooling the fct martensite begins to form starting at about 60$^{o}$C. The film stress continues to drop off rapidly while the transformation proceeds. During subsequent thermal cycling, the stress vs. temperature curve follows that of the first thermal cycle, validating the thermoelastic nature of the fcc to fct transformation in this film.

Metallic films deposited on Si substrates typically exhibit a decrease in tensile stress with increasing temperature. The coefficient of thermal expansion of a metallic material is several times larger than that of Si. Therefore, the stress in the metallic film becomes more compressive with increasing temperature as the metal tries to expand more than the underlying Si substrate.

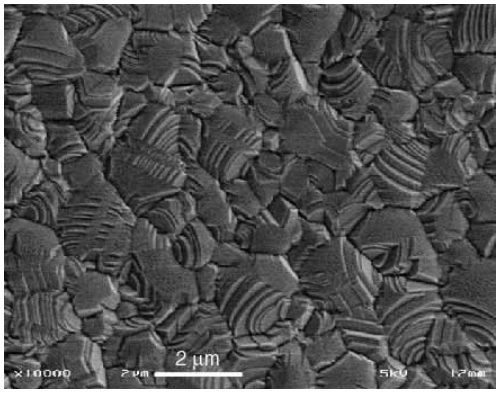


**Figure 5.** SEM micrograph showing the grain size and the surface morphology of the film after heat treatment at 900$^{o}$C for 15 minutes in oxygen-gettered flowing Ar. The Pd content in this sample is 28.8 at.% and the film thickness is 580 nm. XRD data indicates absence of iron oxide in this sample (see Figure 4).

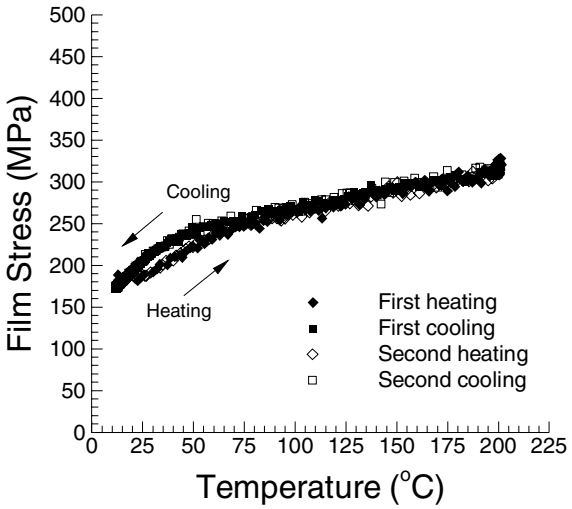


**Figure 6.** Changes in film stress as a function of temperature in a sample containing some fct martensite at room temperature (28.56 at.% Pd).

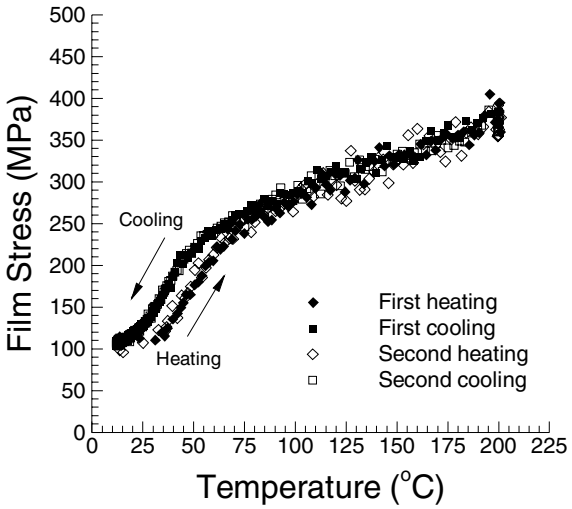


**Figure 7.** Changes in film stress as a function of temperature in a sample containing fct martensite at room temperature (28.3 at.% Pd).

Figures 6 and 7, however, show an opposite trend after the film transforms to the fcc austenite phase. This phenomenon can be attributed to the existence of anomalously low values of coefficients of thermal expansion in Fe-Pd alloys containing approximately 30 at.% Pd [15]. This invar-like behavior observed in the sputter deposited Fe-Pd thin films will be discussed in a separate paper [16].

The fct martensite in bulk Fe-Pd alloys is known to exist in a very narrow composition range at low temperatures. However, as shown by the film stress measurements above, in thin films the temperature range over which the fct martensite exists can be raised above room temperature. This experimental observation of increased $M_s$ in the presence of a tensile stress is consistent with the Clausius-Clapeyron equation. Furthermore, this trend is also consistent with the results obtained by Kato et al. [10] in which stress-induced fct martensite was obtained in bulk polycrystalline Fe-30.5 at.% Pd samples at elevated values of $M_s$. The ability to obtain the fct martensitic phase at near room temperature enables realization of Fe-Pd shape memory thin films in practical applications.

## CONCLUSIONS

Fe-Pd shape memory thin films with approximately 28 at.% Pd were successfully deposited by magnetron sputtering from elemental Fe and Pd targets. Post deposition heat treatment at 900°C for 15 minutes in flowing Ar followed by rapid cooling in flowing Ar produces the metastable fct martensite at room temperature. Existence of the shape memory effect in this material was confirmed by the changes in film stress under thermal cycling. Characterization of the magnetic properties of the film as well as the study of the shape memory effect in the presence of an externally applied magnetic field will be topics of future investigation.

## ACKNOWLEDGEMENTS

This work was funded by Center for Imaging and Mesoscale Structures (CIMS) Seed Money Program at Harvard University. T. Cohen-Karni was supported on Research Experience for Undergraduates (REU), a MRSEC program funded by the NSF.

## REFERENCES

1. K. Ullakko, J.K. Huang, V.V. Kokorin and R.C. O'Handley, *Scripta Mater.* **36**, 1133 (1997).
2. Y. Liang, H. Kato, M. Taya and T. Mori, *Scripta Mater.* **45**, 569 (2001).
3. K. Inoue, K. Enami, Y. Yamaguchi, K. Ohoyama, Y. Morii, Y. Matsuoka and K. Inoue, *J. Phys. Soc. Jpn.* **69**, 3485 (2000).
4. T. Sakamoto, T. Fukuda, T. Kakeshita, T. Takeuchi and K. Kishio, *J. Appl. Phys.* **93**, 8647 (2003).
5. T. Kakeshita, T. Takeuchi, T. Fukuda, T. Tsujiguchi, T. Saburi, R. Oshima and S. Muto, *Appl. Phys. Let.* **77**, 1502 (2000).
6. R.D. James and M. Wuttig, *Phil. Mag.* **A77**, 1273 (1998).
7. M. Sugiyama, R. Oshima and F.E. Fujita, *Trans. JIM.* **25**, 585 (1984).
8. Y. Furuya, N.W. Hagwood, H. Kimura and T. Watanabe, *Mater. Trans. JIM*. **39**, 1248 (1998).
9. Y. Liang, T. Wada, H. Kato, T. Tagawa, M. Taya and T. Mori, *Mater. Sci. Eng*. **A338**, 89 (2002).
10. H. Kato, Y. Liang and M. Taya, *Scripta Mater.* **46**, 471 (2002).
11. Z. Wang, T. Iijima, G. He, T. Takahashi and Y. Furuya, *Int. J. Appl. Electromag. Mech.* **12**, 61 (2000).
12. Z. Wang, T. Iijima, G. He, K. Oikawa, L. Wulff, N. Sanada and Y. Furuya, *Mater. Trans. JIM*. **41**, 1139 (2000).
13. S. Inoue, K. Inoue, K. Koterazawa and K. Mizuuchi, *Materi. Sci. Eng*. **A339**, 29 (2003).
14. S. Inoue, K. Inoue, S. Fujita and K. Koterazawa, *Mater. Trans. JIM.* **44** 298 (2003).
15. M. Matsui, T. Shimizu and K. Adachi, *Physica* **119B**, 84 (1983).
16. Y. Sugimura, T. Cohen-Karni, P. McCluskey and J. Vlassak, manuscript in preparation.